2004

Planar Magnetics Design For Low-voltage Dc-dc Converters

Shangyang Xiao
University of Central Florida

STARS Citation

Showcase of Text, Archives, Research & Scholarship

PLANAR MAGNETICS DESIGN FOR LOW-VOLTAGE
DC-DC CONVERTERS

by

SHANGYANG XIAO
B.S. Beijing Institute of Technology, 1995

A thesis submitted in partial fulfillment of the requirements
for the degree of Master of Science
in the Department of Electrical and Computer Engineering
in the College of Engineering and Computer Science
at the University of Central Florida
Orlando, Florida

Summer Term
2004

ABSTRACT

The objectives of this thesis are to design planar magnetic devices based on accurate electromagnetic analysis and miniaturize magnetics within desired low profile as well as small footprint. A novel methodology based on FEM simulation is proposed. By introducing Maxwell 2D simulator, optimal interleaving structures can be found to reduce AC losses that cannot otherwise be accounted for by conventional method. And 3D simulator is employed to make the results more realistic. Thus, high-efficiency high-power density magnetics is achieved.

ACKNOWLEDGMENTS

First of all, I would like to express my heartfelt appreciation to Dr. Thomas X. Wu for being my advisor and shepherding me into electrical engineering area. His imagination, integrity, and vast knowledge have been an invaluable resource to me. I would have been lost without his continuous guidance, support, and encouragement.

Thanks go to Dr. Issa Batarseh for helping me develop my background in power electronics. Besides, I'd like to thank Dr. Kai Ngo who is with University of Florida, for his many valuable comments, wise advice, and discussions on my research work.

I am so indebted to all members from the Electromagnetics and High Speed Electronics group, and Florida Power Electronics Center. The friendship, enlightening discussions, and overall group spirit have benefited my study and stay at UCF.

TABLE OF CONTENTS

LIST OF FIGURES

vi

LIST OF TABLES

1 INTRODUCTION

The increasing demand of smaller-size and cost-effective DC/DC converters has expected design engineers to develop power converters capable of operating at higher switching frequencies with high efficiency. However, even with modern advanced topologies, magnetics is still one of the biggest challenges in achieving higher power density and higher efficiency due to the significant portion of magnetics in the whole power system [1].

In recent years, there have been two distinct trends in magnetics design in power electronics systems. The first trend concerns the use of planar structures [2], with which much closer board spacing and lower profile can be achieved. Easier manufacturability due to the simpler conductor assembly methods makes planar structures prevailing in the power converter industry. The second trend is to move continuously toward higher frequencies in order to reduce the size of magnetic components. Currently the mature frequency for switched-mode power supplies (SMPS) is around 200 kHz; several hundreds of kilohertz systems are being extended; and there is also a push of switching frequencies to several-megahertz range [3]. However, the design of transformers and inductors is usually a limiting technology for such higher frequencies.

Additionally as an approach to accomplish low profile and high power density in power applications, integrated magnetics is investigated intensely in the past decades. With integrated magnetic techniques, several magnetic components can be constructed in one magnetic core by sharing a common magnetic path. Therefore, the number of magnetic cores is reduced, and the flux ripple may also be suppressed [4, 5].

1

Since the magnetic components usually occupy a large portion of size in a power converter, an optimal design of transformers and inductors thus becomes critical to miniaturize the system profile and further increase its power density. For conventional approaches, magnetic components are often designed based on magnetic-circuit models. Core loss and conduction loss in magnetic devices are roughly estimated. However, with the increase of switching frequency driven by continuously lower profile and higher power density, traditional analysis makes it very difficult to evaluate the loss due to skin effect and proximity effect. Therefore an innovative methodology based on numerical analysis of electromagnetic fields is desired.

So far there is little research work done in modeling magnetics in a wider frequency range for power converters based on the analysis of electromagnetic fields. Being one of the most popular tools for electromagnetic design in industry, Ansoft Maxwell Field Simulators (Maxwell 2D and 3D) have shown their powerful capability of electromagnetic computations with unsurpassed accuracy and ease of use, which stimulates their prevalence in magnetics design.

In this thesis, design issues of planar magnetics, including loss mechanism in copper and core, winding design on PCB, core selections, winding arrangements and so on are firstly reviewed. After that FEM simulators are introduced to numerically compute the winding loss. Consequently, a software platform for magnetics design is established. Wherein spreadsheets are employed to determine the layer arrangement that minimizes the overall DC loss, and Maxwell 2D is introduced to simulate topologies of proposed magnetics, hence Maxwell 3D is employed to optimize the results for its accuracy. From the computed electromagnetic fields, conduction

loss can be accurately evaluated for each of the winding structures, and optimized magnetics can then be achieved.

2 REVIEW ON PLANAR MAGNETICS TECHNOLOGIES

2.1 Planar Magnetics Structures

The drive towards higher power density with overall lower profile in switched-mode power supplies has exposed a number of limitations in the use of conventional magnetic structures. However for conventional wire wound magnetic components, this led to problems of increased loss due to the skin and proximity effects in the round conductors particularly at frequencies above 100 kHz. The earlier applications of planar magnetics demonstrated the use of flat wide conductors to decrease skin and proximity losses in windings compared to round wire [6-9], and illustrated the control of other parameters like leakage inductance. The repeatability of component characteristics also proved of considerable importance, particularly for use in resonant converters in the 1-10 MHz range [10, 11].

Windings of planar magnetics are essentially formed using common interconnection technologies, such as printed circuit boards (PCBs), thick film and flex. Many early designs used thick film technology [10, 12-14] for the realization of the windings but by far the most popular approach was the use of PCB, flex or stamped copper turns. The early 90's saw many investigations into the characteristics, modeling and optimization of planar magnetics [15]. The disadvantages of using non-standard low profile cores were addressed in the mid 90's when core manufacturers introduced ranges of standard planar cores, e.g. planar EE and EI cores, and low

profile versions of conventional cores, e.g. RM cores. More recently planar ER and EIR cores have been introduced, thus contributing to the more widespread acceptance of planar magnetics.

Typical planar magnetic structures compared to the traditional wire wound magnetics with applications in power electronics are shown in Figure 2.1.
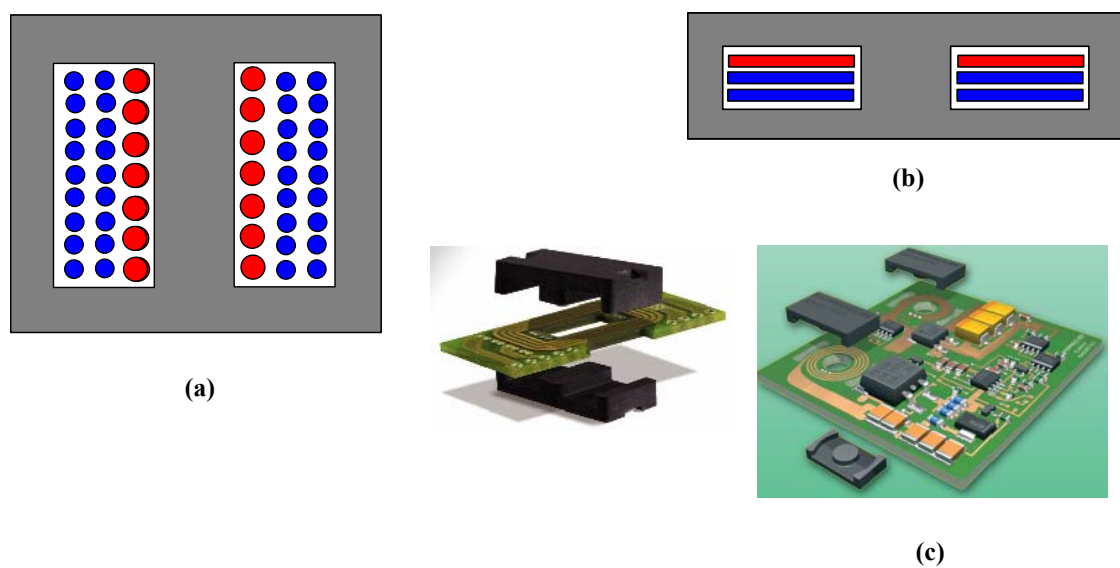
Figure 2.1 Magnetics structures: (a) conventional structure; (b) planar structure; and (c) applications of multi-layer PCB magnetics (www.ferroxcube.com).

Obviously the core of the planar device has a lower profile than that of the conventional device. Also, windings on the conventional device are stacked so that they are successively further from the center leg, i.e. windings are built up in the horizontal dimension while on the planar device they are stacked in the vertical direction instead.

2.2 Characteristics of Planar Magnetics

Since multi-layer PCBs allow the interconnection of arbitrary layers, interleaved primary and secondary windings can be implemented much more easily than conventional magnetics. This provides the means to further reduce leakage and high frequency winding losses [16], both of which have obvious advantages for high frequency square wave switching. A further advantage of the planar magnetics is the enhanced thermal performance possible because of the greater surface area to volume ratio, thus providing more area to contact the heat sink. This is illustrated in the smaller value of thermal resistance quoted for planar cores over conventional cores [17].

The characteristics of planar magnetics are, of course, not all advantageous. In particular the planar format, although improving thermal performance, increases footprint area. The fact that windings can be placed close together thus reducing leakage inductance has the usually unwanted effect of increasing parasitic capacitances. The repeatability of characteristics obtained from PCB windings also comes at the price of having a greater portion of the winding window filled with dielectric materials, thus reducing copper fill factor and limiting the number of turns. Another main disadvantage of planar transformers is that most of the procedures to build them are complex and expensive. Further more, typical problems of planar structures are the thermal management and the high value of capacitive effects. However, in many applications, it is still advantageous to use multi-layer PCBs in planar magnetics.

2.2.1 Low Profile

An important feature of planar transformers is their low profile. This feature makes almost necessary the use of planar transformers in on-board converters. The term *low profile* is often used to describe planar magnetics. However, not all low profile magnetics are planar. In particular low profile cores, such as the EFD type, use conventional wire wound technology, lacking many of the characteristics of planar magnetics.

The effect of core height on power density has been studied in several references [1, 18-20]. In particular, some of these studies have compared planar magnetics to more conventional low profile magnetics and found that the low profile magnetics can have better volumetric efficiency [19] and higher power density for certain applications [20].

2.2.2 High-Frequency Losses

Some earlier studies assessed winding configurations [16, 19], investigated the optimum placement of windings [21], compared different winding technologies [16] and optimized the layout of turns to minimize overall DC winding resistance [22].

In an analysis of different winding configurations involving the use of solid wire, Litz wire, PCB and foil windings at 500 kHz, PCB windings have lower AC resistance (approximately 85–90%) than similar solid wire windings but higher than Litz wire windings

(approximately 115%) [16]. Leakage inductances of the PCB implementations are lower than both the wire and Litz wire implementations.

It also became evident that circularly wound planar windings can have significant 2D field effects in the winding window [19], which gives rise to losses not accounted for by the traditional approach to the winding loss computation [23]. These effects were also investigated for foil windings and conclusions drawn as to how these 2D or *edge effects* might be minimized [21]. The conclusions were that winding losses were minimized for primary and secondary layers with equal width, and for minimum spacing between winding end and core center leg.

2.2.3 Leakage Inductance

The ease with which interleaving can be implemented in planar structures allows the minimization and control of leakage inductance within the windings [16, 24].

However, since the leakage inductance of planar components can be so low, particular attention should be paid to the termination of the windings. For example, depending on the secondary termination method used, the leakage inductance presented to the circuit can be up to three times that computed by the classical short circuit secondary approach.

It is obvious that the benefits of careful transformer design can easily be nullified by a lack of care in the connection of the transformer to the rest of the circuit. Inappropriate termination design can also account for as much as 75% of the short circuit AC resistance of a planar device [16].

2.2.4 Planar Winding Technologies

Various technologies can be used to implement the planar windings. The most popular of these have been compared in the literature [16], i.e. printed circuit board (PCB), flex circuit and stamped copper. Windings fabricated in thick film and LTCC have also been used primarily in lower power applications. In this thesis, the design of magnetics will mainly focus on PCB structures.

The use of PCBs gives a highly repeatable and manufacturable means of implementing planar windings. In principle, the windings can be an integral part of the system interconnection substrate thus totally eliminating all terminations. However, in practice the interconnection substrate rarely has sufficient layers to fully accommodate the magnetic component windings. The disadvantage of PCBs is that the window utilization factor can be quite low (typically 0.25 - 0.3 compared to 0.4 for conventional magnetics) due to a typical inter-turn spacing of 150 μm and minimum dielectric thickness of 100 μm.

Flex circuit (copper on a thin, flexible polymer substrate) gives an improved utilization factor, as the dielectric thickness is as low as 50 μm. Many layers of flex circuit can be laminated together resulting in a rigid structure similar to a PCB but with increased utilization factor. Alternatively, it can facilitate the use of techniques such as the "z-folding" method. This folding method can be used to implement a large number of layers without the need for vias or soldering for layer interconnects. Similar to PCBs, flex conductor thickness may be limited to standard thickness, typically 17, 35, 70, and 105 μm, with minimum conductor spacing increasing with

increasing thickness. Unlike PCBs, the flex technologies are more suitable to much heavier copper weights, e.g. 210 μm or larger.

Stamped copper windings provide a low cost means to implement high current, thick, and single turn windings. The main disadvantages are that insulation layers must be separately applied and layer interconnection provided by some external means.

2.3 Planar Cores

Cores for planar components come in several forms, as shown in Figure 2.2.

| (a) | (b) | (c) | (d) |
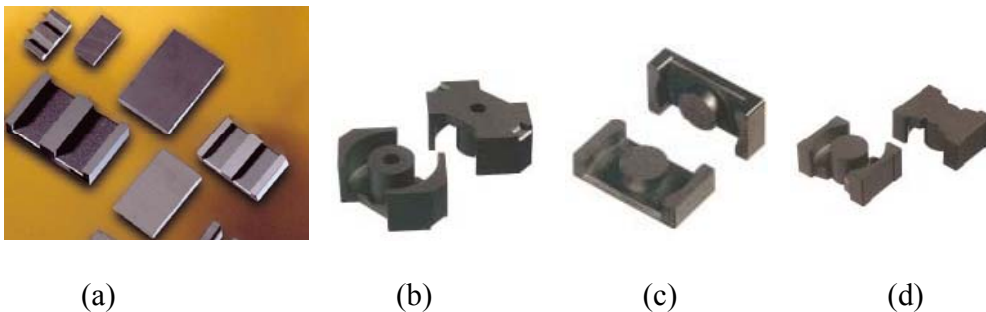
Figure 2.2 Typical planar core shapes: (a) EE and EI cores; (b) RM cores; (c) ER cores; and (d) PQ cores.

Probably the most popular is the planar EE or EI core, specifically designed for planar magnetics and now offered by most manufacturers in several industry standard sizes. Other planar cores include low profile versions of standard cores such as RM, ER, PQ and so on. Because of its rectangular center leg, the EE core requires the use of a relatively long turn which

must extend a considerable distance beyond the core, thus giving rise to issues of space usage and possibly EMI. Cores with circular center legs such as RM, ER, PQ, etc. allow for shorter turns, and possibly improved shielding. However most of these low profile cores have a smaller winding window area to core area ratio than the EE core, thereby limiting the number of winding turns.

It is interesting to note that optimization studies on planar components have shown that there exists an optimal component height which maximizes power density for any set of specifications [18] and that higher power densities can be achieved by using custom cores [19]. Thus the limited range of standard planar cores is unlikely to offer the optimum solution for a particular design, so that if cost constraints permit, custom core designs should be investigated to maximize performance.

2.4 Applications in Power Electronics

The application of planar magnetic structures is wide-ranging across power levels and magnetic functions. The common characteristics of these structures have been discussed in the previous section. This section concentrates on the desired characteristics that are application dependent.

2.4.1 Power Transformers

Planar transformers designed for power applications must satisfy the same requirements as conventional power transformers including the minimization of loss mechanisms and the provision of an acceptable cooling strategy. The task of minimization of the core losses is similar to that of a conventional wound magnetic. It requires suitable choices of the switching frequency, core shape and size and core material. The main difference lies in the choice of core shape and size.

Minimizing copper losses at high frequencies requires a good understanding of the principles of skin effects and proximity losses. Interleaving is a well-known technique used to minimize high-frequency effects contributing to winding losses within planar turns. However, the level of interleaving is limited by the considerations of capacitive effects and the concerns of providing adequate levels of isolation between the windings. Application of these principles means that filling the core window with copper is usually not the best solution. In fact, in many applications high levels of interleaving of relatively thin layers results in a high insulator to copper cross-sectional ratio. This makes the use of printed circuit boards particularly suitable for transformer winding structures despite the upper limit of approximately 45 to 50% on copper utilization of the window. In some very low profile applications, the copper utilization factor can be increased through the use of thinner insulation systems. In the case of single-turn, single-layer secondary windings designed to carry high current, thick external copper stampings can augment or replace PCB layers. In some applications where further interleaving is undesirable or not practical, thicker copper may be used for improved thermal transfer without a loss or efficiency

penalty. It must be noticed that, reductions in leakage inductance and winding resistance can be offset by poor termination design resulting in a poorly designed transformer [16].

2.4.2 Power Inductors

Depending on the application, the requirements of planar power inductors can be very similar or very different to those of power transformers. For simplicity we limit our discussions to two categories. The first category is inductors where the ripple current is a small percentage of the average dc current component (say, less than 5% on an RMS basis). The other category is where the ripple current is large relative to the dc component (say, greater than 20%). Of course, many applications are somewhere in between and tradeoffs are required.

In the case of small ripple, we can assume that current is a dc current and that skin effect and core losses can be ignored. The design of the planar inductor then reduces to choosing the lowest resistance winding possible based on the constraints of the core size and gap. Minimizing the number of turns on the inductor is the first step towards achieving a low winding resistance. The next and, probably, more difficult challenge is to maximize the copper utilization of the core window.

Other approaches to implementing windings on a low profile planar magnetic core involve incomplete turns (often called staples). The turns are completed by copper etch on the converter's PCB.

For inductors where the ac ripple content is high, the design of the winding has issues very similar to that of transformer winding design with one more difficulty. There is usually no secondary winding that can be used to reduce proximity effects through interleaving.

With regard to core design, there is now a significant ac flux component causing core losses and potentially contributing to eddy-current losses if the gap and the winding are in close-proximity. This is not an unreasonable assumption in planar devices as two of the primary goals are small size and high power density. In these cases, a lumped gap may result in unacceptably high losses in the winding and alternative-gapping strategies (e.g. distributed gaps) may merit consideration.

2.4.3 Integrated Magnetics

A discussion of planar magnetics would not be complete without the consideration of integrated magnetics structures.

These devices combine multiple magnetic functions on a single core structure. With the exception of the fly-back transformer and some coupled-inductor applications, integrated magnetic devices have been slow to gain widespread use in the power supply industry. While these devices offer many advantages, e.g. reduced parts count and improved performance, potential gains have usually been offset by the complexity of the winding structures and the associated cost.

The maturing of the technologies associated with planar devices has helped overcome some of these complexities and the associated costs. Examples now abound where the advantages of planar devices have allowed the practical implementation of magnetic structures that were previously very difficult or unfeasible. The advantages range from repeatability and reproducibility, which help control manufacturing cost, through improved thermal performance and the minimization of interconnections between devices. The minimization of interconnects is obviously very advantageous in low voltage high current applications for efficiency reasons.

Some converter topologies are well documented and analyzed for their applicability to planar technologies. Most of these suitable topologies appear to have an obvious symmetry from the perspective of the magnetic devices, e.g. push-pull primaries, current-doubler secondaries and center-tapped secondaries.

However, not all converter topologies are necessarily suitable for planar magnetic integration, such as the integration of the isolating transformer and the output inductor of the forward converter. The optimization of this device can severely compromise the low-profile feature of planar devices. The evolution from discrete devices to integrated magnetic structure on a three-legged core is well documented. Optimization of this structure is somewhat problematic when planar magnetics are considered. For example, one option is to locate the transformer windings on the outer legs and the inductor winding on the center leg. While this results in a symmetric structure, the magnetic path length associated with the transformer, and its large ac flux content, can be very long resulting in high core losses. The need for a wide (i.e. low resistance) inductor winding exacerbates this problem by further increasing the magnetic path length. The other option is to locate the transformer windings on adjacent legs and locating the

inductor winding on an outside leg. Unfortunately, flux splitting no longer occurs and if window height is to be maintained the core height will have to grow. Thus, the low-profile advantage of planar structures is immediately compromised.

Some of these issues have begun to be addressed through the use of multi-chambered structures. A stacked multi-chamber approach appears to be very flexible from a design standpoint but probably has limited usefulness in low profile applications. The side-by-side (or concentric) approach appears most promising for low-profile applications but access to the inner windings could be problematic especially for surface-mount applications.

2.5 Modeling and Design

As we have seen in Figure 2.1, the main difference between conventional and planar magnetic devices is in terms of their winding structures. Consequently models for predicting components of impedance for conventional windings are not accurate when applied to planar structures. This is particularly true for components of winding resistance and leakage inductance.

New methods to model planar structures include analytical and numerical techniques. A 1D analytical formula is widely used for modeling high frequency losses in conventional windings [23] although significant errors are possible. The formula is based on an assumption of uniform magnetic fields along the height of the core window, and losses are calculated in each radial winding layer. However, due to the small window utilization factor in planar structures, significant 2D fields link within the wide conducting sections and cause much higher losses than

predicted by 1D solution. The development of commercial software simulation tools based on numerical techniques has increased the popularity of this approach. 2D numerical analysis approaches can further improve the loss estimations in planar structures.

Leakage inductance can also be predicted from 1D analytical method, but again numerical techniques are more effective for investigating high frequency effects contributing to leakage fields in planar structures. It has been proved that the values of leakage inductance may be severely underestimated by 2D models [24]. Differences have been found to be due to leakage fields associated with terminations used to shorten the secondary terminals during measurement. That is, leakage inductance within the planar winding structure is often small enough that it is comparable to that contributed by external shorting connections. As an example in [1], measurements performed on a 100 W transformer design are compared with results predicted by 2D and 3D finite element analysis (FEA) of the structure under short circuit conditions. It is shown that inclusion of the shorting connection between secondary terminals in the 3D model accounts for a high percentage of total leakage inductance where the measured leakage inductance is over 6 times larger than predicted by 2D FEA. In fact, the 3D FEA modeling overestimates the leakage effects (approximately by 28%). Obviously, a 3D model must be applied to include the effect of such terminations.

3 MAGNETICS DESIGN ON MULTI-LAYER PCB

3.1 Loss Mechanisms in Magnetics

The total power loss in magnetic devices usually consists of core loss in magnetic materials and copper loss in windings. The core loss has two portions, which are hysteresis loss and eddy current loss while the copper loss is often explained by DC or AC power loss dissipated in the windings in the form of heat.

3.1.1 Core loss

Consider an *n*-turn inductor excited by periodic waveforms *v(t)* and *i(t)* having frequency *f*, the net energy that flows into the inductor over one cycle is [25]

$$
\begin{aligned}
W &= \int_{onecycle} v(t)i(t)dt \\
&= \int_{onecycle} \left(nA_C \frac{dB(t)}{dt} \right)\left(\frac{H(t)\cdot l_m}{n} \right)dt \\
&= \left(A_C l_m \right) \int_{onecycle} HdB
\end{aligned}
\tag{3.1}
$$

and the hysteresis loss is

$$
P_H = \left(f \right)\left(A_C l_m \right) \int_{onecycle} HdB
\tag{3.2}
$$

On the other hand, ferrites, as widely used magnetic core materials in power electronics systems, usually are good electrical conductors. Consequently ac magnetic fields can cause electrical eddy currents to flow within the core material itself, as shown in Figure 3.1. Eddy current losses contribute significantly in the total core losses at high frequencies.
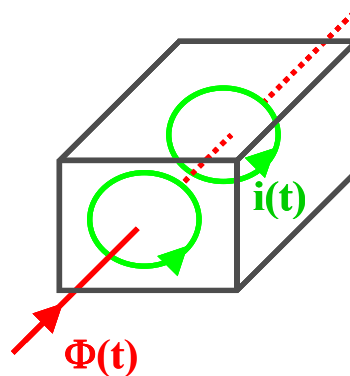

Figure 3.1 Eddy currents in a magnetic core.

To accurately evaluate the core loss resulting from hysteresis loss and eddy-current loss in magnetic cores, Philips has developed software that can give core loss density P_V at different temperatures for arbitrary flux waveforms of inputs. Figure 3.2 contains core loss data samples for Ferroxcube 3C96 ferrite material.
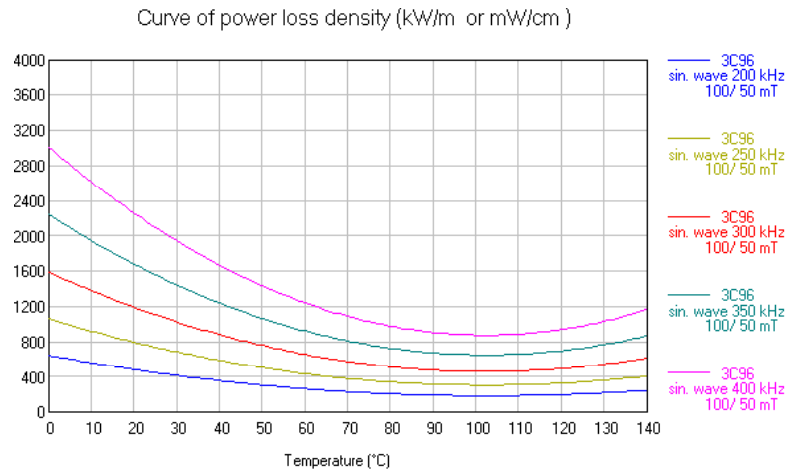
Figure 3.2 Core loss data samples for 3C96 ferrite material.

At a given frequency *f*, the core loss P_{core} can be approximately expressed by an empirical function of the form [25]

$$P_{core} = K_{fe}(\Delta B)^{\beta} A_C l_m = P_V V_e \tag{3.3}$$

where P_v is obtained from Philips software and V_e is specified by vendors. It is obvious that core loss is proportional to core size and increases as frequency goes high. However, the relationship between core loss and temperature is not uni-directional. As shown in Figure 3.2, there exists a minimum core loss point at a specific temperature.

3.1.2 Copper Loss

The DC or low-frequency copper loss in the windings can be estimated by

$$P_{Cu} = I_{rms}^2 R_{DC} \tag{3.4}$$

where I_{rms} is the RMS value of the current flowing through the windings, and the dc resistance can be expressed as

$$R_{DC} = \rho \frac{l_b}{A_W} \tag{3.5}$$

where A_W is the wire bare cross-sectional area, l_b is the length of the wire, and ρ is the resistivity of copper.

At high frequencies, eddy currents in the windings due to skin effect and proximity effect also cause power losses, and usually lead to copper loss significantly in excess of DC or low-frequency loss expressed above.

One way to reduce the high-frequency loss due to skin effect is to decrease the thickness of conductor to the order of one skin depth such that the ac current can be assumed to be uniformly distributed in the cross-sectional area of the winding. For a planar magnetic structure, since the thickness of the conductor is usually comparable to one skin depth, the skin effect can be suppressed. For example, the thickness of 4-oz PCB is about 140 μm while the penetration depth (or skin depth) for the copper at 400 kHz is about 104 μm. From circuit point of view, it is usually reasonable to ignore the skin effect when the thickness of copper is less than twice of the skin depth. For most of planar copper structures, however, the currents are distributed

dominantly in the two ends rather than on the surface evenly. Figure 3.3 illustrates an example of skin effect from electromagnetic simulation.
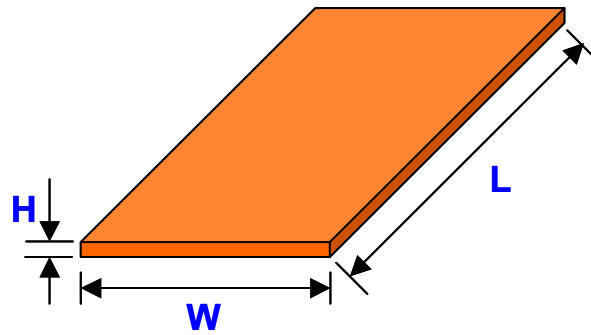
(a)
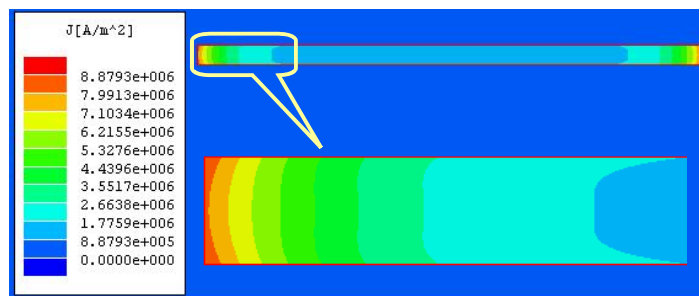
(b)

Figure 3.3 Skin effect in a 4-oz PCB copper trace (H=140 μm, W/H=25): (a) Copper configuration, and (b) current distribution.

On the other hand, proximity effect also contributes much to the total high-frequency loss as shown in Figures 3.4 and 3.5.
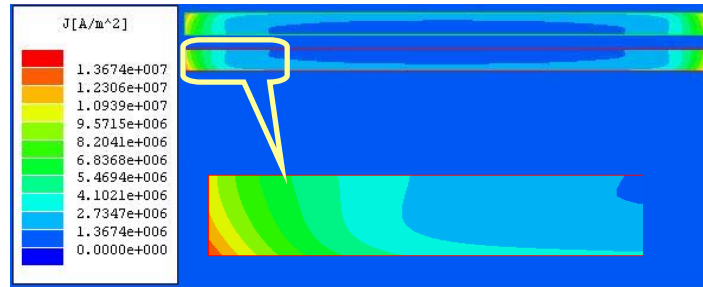
Figure 3.4 Proximity effect (two layers in parallel).

Figure 3.5 Proximity effect (three layers in parallel).

From Figures 3.3 to 3.5, it is obvious that the distribution of ac currents is no longer uniform in the planar windings. Therefore the accurate ac resistances can be computed only from EM simulation (like FEA). Table 3.1 lists the ratio of ac resistance to dc resistance for each case above at frequency of 400 kHz.

Table 3.1 AC resistances due to skin effect and proximity effect.

	R_{ac}/R_{dc}
One single copper layer	1.59
Two layers	2.24
Three layers	2.22

One way to reduce the copper losses due to the proximity effect is to interleave the windings (especially for transformer design). Figures 3.6 and 3.7 explain how to improve current distribution and therefore reduce total ac loss by interleaving primary and secondary windings in power transformers.
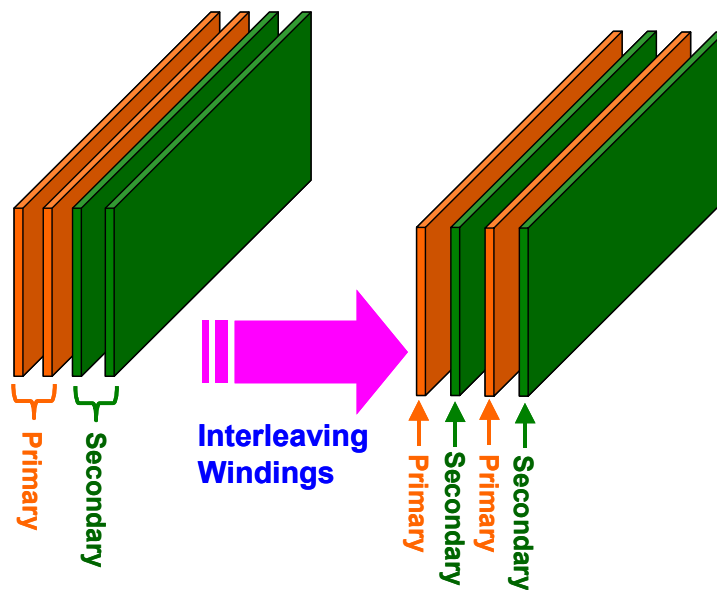
Figure 3.6 Interleaved windings.
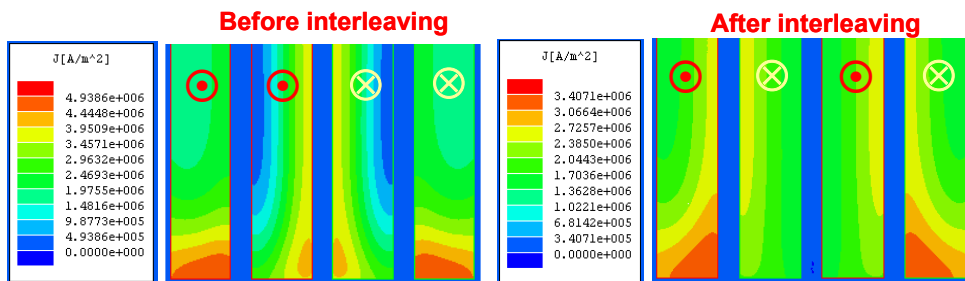
Figure 3.7 Current distributions before and after interleaving.

Apparently the current is distributed more uniformly after interleaving the primary and secondary windings. As a result, the ac loss can be reduced.

3.2 Design of Planar Transformer

3.2.1 Specifications

As an example, we will design a planar transformer using 8-layer PCB with low profile of 0.22 inch, output power of 60 W, and high frequency of 88% for the DCS-PWM-based ZVS converter [26]. Figure 3.8 shows the topology of the DCS-PWM-based ZVS converter with the specifications given in Table 3.2.
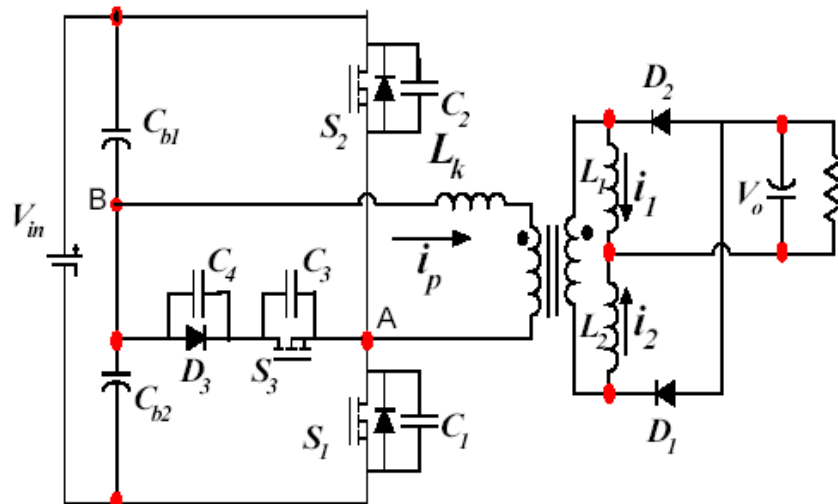
Figure 3.8 DCS-PWM-based ZVS topology [26].

Table 3.2 Specifications of the converter.

Input voltage (V)	36~75
Output voltage (V)	1.2
Output power (W)	60
Efficiency@ full load	88%
PCB layers	8
Copper thickness (mm)	0.14
Insulation thickness (mm)	0.11

The voltage waveform for the primary winding is shown in Figure 3.9.
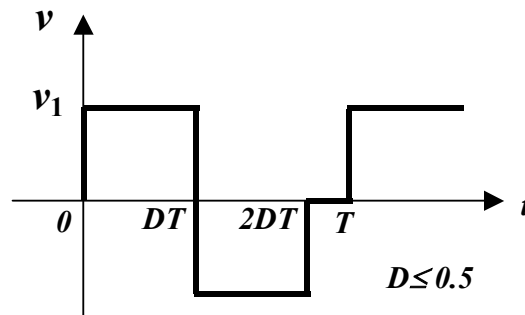
Figure 3.9 Voltage waveform for the primary side of the transformer.

The design specifications for the transformer are given in Table 3.3.

Table 3.3 Design specifications for the transformer.

Primary voltage (V)	18~37.5
Turns ratio	4
Switching frequency (kHz)	400

The design platform can be described as shown in Figure 3.10. The core materials and core shapes are first selected. Then Philips software is used to calculate the core losses. In terms of converter-dependent excitations, window partition between primary and secondary windings can be accomplished. Then, Maxwell 2D simulation gives the optimal interleaving structures and winding layout is determined by Maxwell 3D simulation. Consequently, total design goal is achieved.
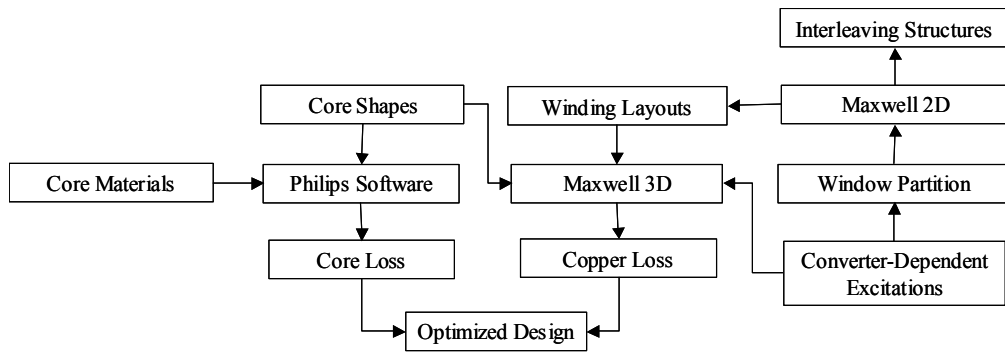
Figure 3.10 Design platform of transformer.

3.2.2 Selections of Core Shape and Material

Since the profile of the magnetics is strictly required to be no more than 0.22 inch, we first look into commercially available planar ferrite cores satisfying such low profile requirement. Three core combinations with less than 0.22 inch profile, as shown in Figures 3.11(a) through (d), may be options for the transformer.
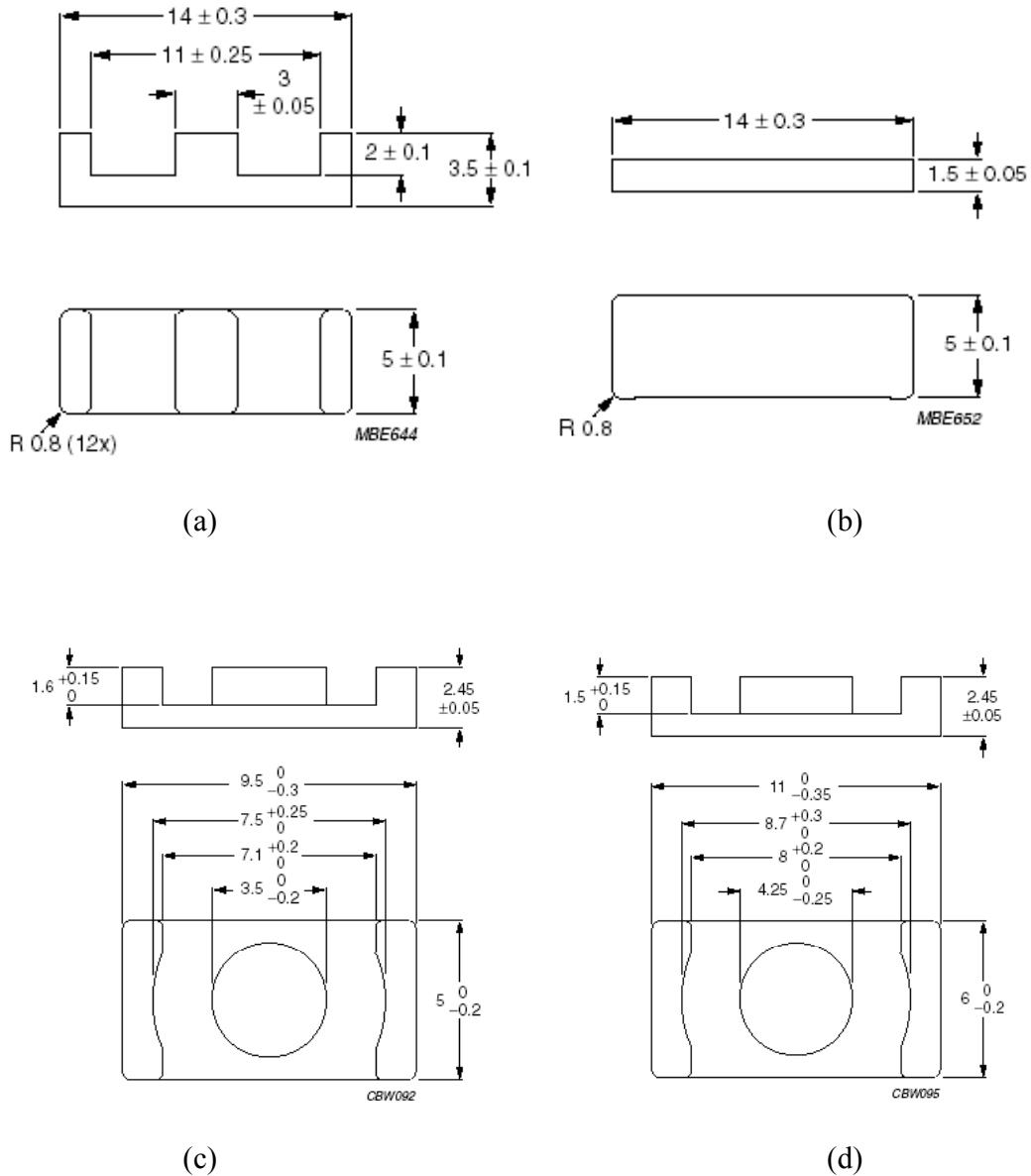
Figure 3.11 Core shapes: (a) E14/3.5/5, (b) PLT14/5/1.5, (c) ER9.5, and (d) ER11.

Although a little bit higher than 0.22" in height, EQ13 can handle larger energy than above cores because of its bigger cross-sectional area. Therefore it is still a candidate core for transformer and inductor. Since the height requirement is mandatory, custom work must be done on EQ13 to satisfy the 0.2" profile. Figure 3.12 shows the core parameters of EQ13.

28

SYMBOL	PARAMETER	VALUE	UNIT
$\Sigma(l/A)$	core factor (C1)	0.911	mm^{-1}
V_e	effective volume	348	mm^3
l_e	effective length	17.5	mm
A_e	effective area	19.9	mm^2
A_{min}	minimum area	19.2	mm^2
m	mass of core set	≈ 0.9	g
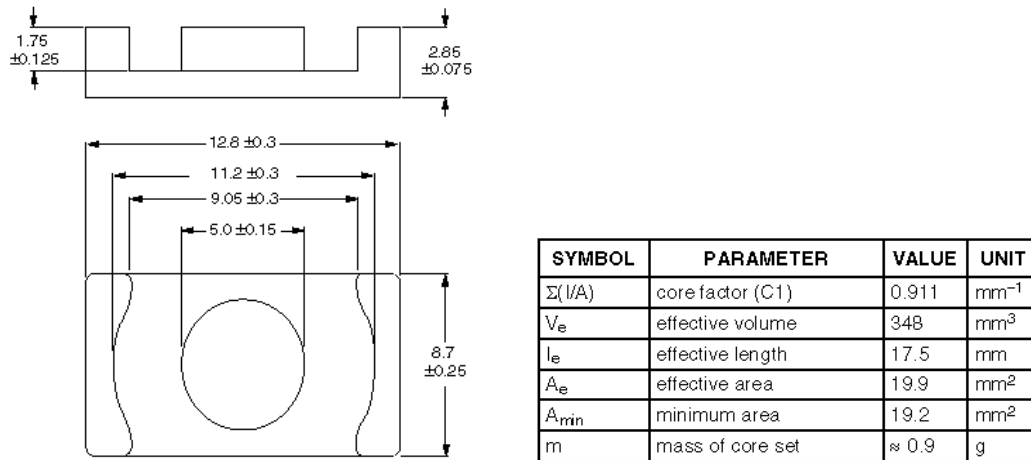
Figure 3.12 EQ13 parameters.

There is always trade off in magnetics design. EQ13 has better performance at the price of increased footprint. Comparisons for the candidate cores are presented in Table 3.4.

Table 3.4 Core shape specifications.

	ER95	ER11	E14	EQ13
Height (mm)	5	4.9	4.9	N/A
A_e (mm^2)	8.47	11.9	14.5	19.9
Footprint (mm2)	47.5	66	70	111.36

The next is to determine turns number for primary and secondary windings, and then evaluate core loss for each core. After that, core material will be selected based on core loss comparison.

From circuit point of view, the turns ratio of the transformer is initially assumed to be 4:1. The numbers of turn for primary and secondary windings are chosen as

$$n_1=4$$

for the primary winding, and

$$n_2=1$$

for the secondary winding.

Therefore, the maximum flux density excited by converter-dependent source can be calculated by the following equation

$$B_{\max} = \frac{\lambda_1}{2n_1 A_C} = \frac{\int_0^{DT} v_1(t)dt}{2n_1 A_C} = \frac{\frac{V_{in}}{2} D \cdot T}{2 \cdot N \cdot A_c} \qquad (3.6)$$

Based on this equation, ac flux densities for these candidate cores are shown in Figure 3.13 at frequencies ranging from 200 kHz to 500 kHz.

Figure 3.13 Sample excitation characteristics.
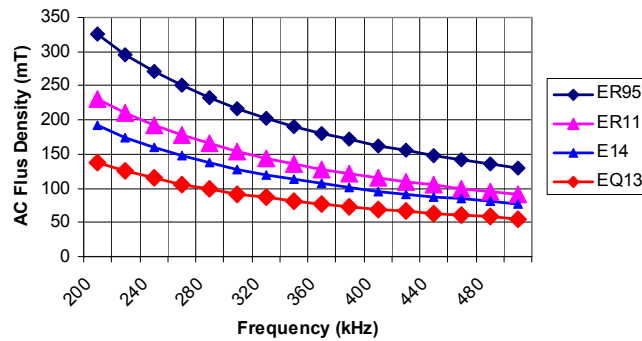
For ferrite 3C96 and 3F35, the saturation flux density is about 300 mT at 100°C. From Figure 3.13, it is obvious that ER95 is not suitable for this work since it saturates at some frequencies. Nevertheless, we will use ER95 for further comparison in the inductor design. By means of Philips software, effects of core materials, shapes, and frequency on transformer core

loss are shown in Figure 3.14, where 3F3 is selected for frequencies less than 400 kHz, and 3F35 is used when frequency is larger than 400 kHz.
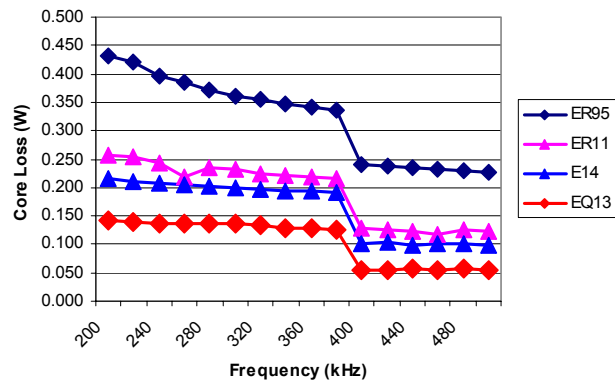
Figure 3.14 Effects of core materials, shapes, and frequency on transformer core loss.

It is also proved that rectangularly wound planar windings have larger fringing field effects than circularly wound windings, and the fringing field effects always give rise to AC losses not accounted for by traditional approach of winding loss computation. Thus E14 may not be a good choice for this work.

By now we have selected the core materials of ferrite 3F3 and 3F35, and core shapes of EQ13 and ER11 for the transformer. In the following, both DC and AC copper losses will be evaluated by Ansoft EM simulation tools. By comparing the copper loss in different interleaving structures, the optimal winding layout is finalized.

3.2.3 DC Loss Estimations

Although the AC loss is usually dominant in the transformer winding losses, it is still necessary to estimate the corresponding DC loss. The skin depth of copper at 400 kHz is 104 μm for 25°C or 120 μm for 100°C and the thickness of 4-oz PCB is about 140 μm that is less than twice of the skin depth. Therefore the DC loss value should basically reflect the AC copper loss if the proximity effect is neglected.

Firstly, we need to determine the dimensions of the PCB trace. The number of turns per layer and the spacing between the turns are denoted by the symbols N_L and S respectively. For an available winding width b_w, the trace width w_t can be calculated from (see Figure 3-15) [27]:

$$w_t = \frac{b_w - (N_L - 1) \cdot S - 2 \times S_1}{N_L} \tag{3.7}$$

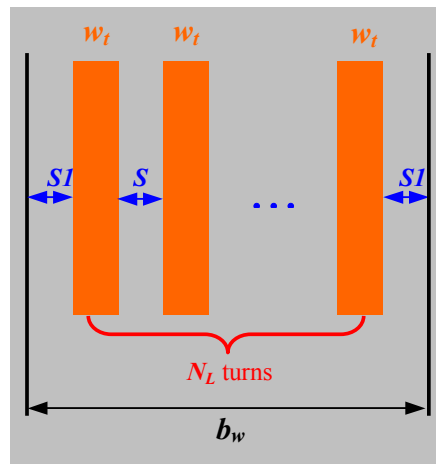
Figure 3.15 Track width w_t, spacing S and winding width b_w

where S_1 and S are specified by the safety rules and fabrication tolerance of industry practice as given below:

$$S_1 = 500 \ \mu m$$
$$S = 300 \ \mu m$$

Since there is only one turn for the secondary winding, the DC loss can be obtained without difficulty. For the primary winding, however, there are several possible winding connections to obtain the desired 4 turns: (a) 4 turns on one PCB layer, (b) 2 turns on one PCB layer and 2 layers in series, and (c) 1 turns on one PCB layer and 4 layers in series. Furthermore, since the PCB has 8 layers of copper trace, more than one layer are arranged for the primary and secondary windings.

After determining the number of turns and dimensions for each layer of the PCB trace, it is possible to estimate the DC copper losses for all arrangements of primary and secondary windings. The calculation results are given in Table 3.5. Since there are two core shapes available, EQ13 and ER11, copper losses are estimated for each core shape.

Table 3.5 Minimum DC loss (W) for each case.

	Case (a)	Case (b)	Case (c)
ER11	1.012	0.387	0.688
EQ13	0.459	0.364	0.294

From the above results, it is found that the minimum DC copper loss for ER11 is the case in which the primary windings are composed of 2 layers in series and each layer has 2 turns. We

simply parallel the other 4 layers for the secondary. For EQ13, the minimum DC loss exists in case (c), i.e., 1 turn is on one PCB layer and 4 layers are in series.

So far we have decided the winding arrangement for the transformer, however, it is usually far away from the optimal design to estimate the copper loss only based on the DC analysis. As stated before, skin effect and proximity effect contribute much to copper loss that is not accounted for by the empirical expression. By properly interleaving the primary and secondary windings, the extra AC loss resulting from proximity effect can be reduced to the largest degree. Therefore, it is critical to quantitatively determine the total AC copper loss for various interleaving winding structures.

3.2.4 Winding Arrangements with AC Loss Simulations

In order to accurately determine the high-frequency conduction loss in transformer planar windings, an effective electromagnetic simulation tool based on finite element analysis (FEA) is usually desired. Ansoft Maxwell Field Simulator (2D or 3D), as one of the most popular software tools in the industry, provides us numerical solutions to the complicated 2D and 3D structures. In the following sections, AC conduction loss in the transformer will be simulated using Ansoft Maxwell Field Simulator.

Since it is always time-consuming to do 3D electromagnetic simulations for complex structures, we will first investigate the current distributions on the cross-sectional area of the windings for various interleaving structures using 2D simulator. By analyzing the current

distribution and conduction loss, the desired interleaving winding structure can be found. Finally accurate AC copper loss may be extracted using Maxwell 3D Field Simulator.

(1) Fourier Transformation of Input

As shown in Figure 3.16, the current waveforms for the transformer are non-sinusoidal, however, Maxwell simulators accept only sinusoidal sources. Thus, significant difference is resulted if using sinusoidal approximation for the inputs. In order to eliminate such effect to a large degree, advanced method is applied to this work.

Let us consider the transmission of energy from a source to a load. If inputs *v(t)* and *i(t)* are periodic, then they may be expressed as Fourier series [25]:

$$v(t) = V_0 + \sum_{n=1}^{\infty} V_n \cdot \cos(n\omega t - \varphi_n)$$
$$i(t) = I_0 + \sum_{n=1}^{\infty} I_n \cdot \cos(n\omega t - \theta_n)$$

$$(3.8)$$

The average power transmitted over one cycle is:

$$P_{av} = \frac{1}{T} \cdot \int_0^T v(t) \cdot i(t) \, dt \qquad (3.9)$$

Let us look into the relationship between the harmonic content of the voltage and current waveforms, and the average power. Substitution of the Fourier series into above equation yields

$$P_{av} = \frac{1}{T} \cdot \int_0^T (V_0 + \sum_{n=1}^{\infty} V_n \cdot \cos(n\omega t - \varphi_n)) \cdot (I_0 + \sum_{n=1}^{\infty} I_n \cdot \cos(n\omega t - \theta_n)) \, dt \qquad (3.10)$$

To evaluate this integral, we must multiply out the infinite series. It can be shown that the integrals of cross-product terms are zero, and the only contributions to the integral comes from the products of voltage and current harmonics of the same frequency:

$$\int_0^T (V_n \cdot \cos(n\omega t - \varphi_n)) \cdot (I_m \cdot \cos(m\omega t - \theta_m)) dt = \begin{cases} 0 & m \neq n \\ \dfrac{V_n \cdot I_n}{2} \cdot \cos(\varphi_n - \theta_n) & m = n \end{cases} \quad (3.11)$$

The average power is therefore

$$P_{av} = V_0 \cdot I_0 + \sum_{n=1}^{\infty} \frac{V_n \cdot I_n}{2} \cdot \cos(\varphi_n - \theta_n) = I_0^2 \cdot R_{dc} + I_1^2 \cdot R_{1ac} + ... + I_n^2 \cdot R_{nac} + ... \quad (3.12)$$

where R_{nac} stands for AC resistance of n-th harmonic. At a specific frequency, I_n can be obtained from Fourier transformation of $i(t)$ (see Figure 3.16), while R_{nac} can be calculated by Maxwell simulator. Through superposition of losses of the dominating components, the total copper loss is obtained.

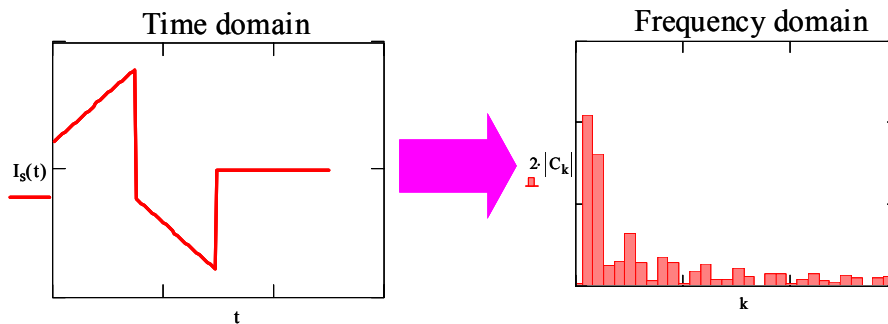Figure 3.16 Fourier transformation

(2) Maxwell 2D Simulations

We consider the structural features of EQ13 and ER11 as shown in Figure 3.17. Axis-symmetrical models are adopted in Maxwell 2D simulation. Figure 3.18 shows the possible winding arrangements for the transformer. The red and green conductors represent primary and secondary windings, respectively.
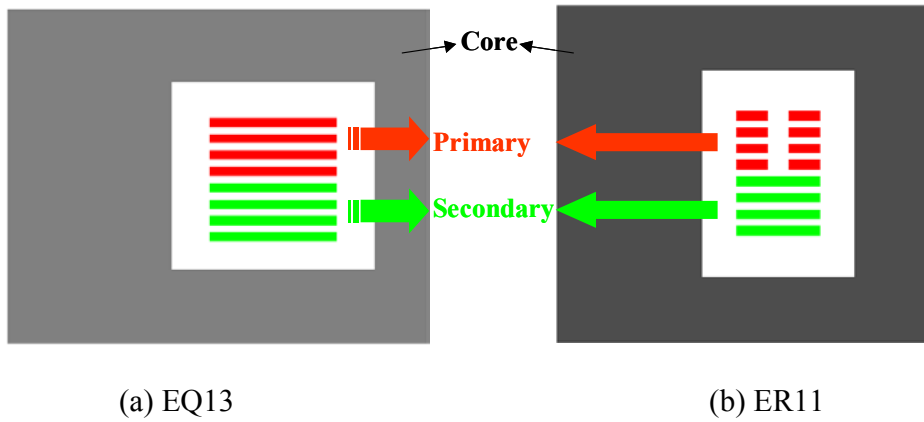
36

(a) EQ13   (b) ER11

Figure 3.17 Winding arrangement without interleaving.

(a) Interleaving structure I;   (b) Interleaving structure II.
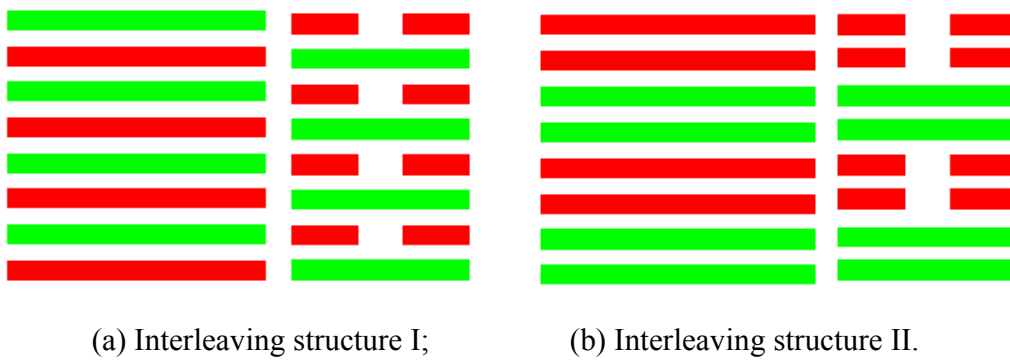
Figure 3.18 Interleaving winding structures for EQ13 and ER11.

Apparently there is no interleaving for primary and secondary windings in Figure 3.17 while two interleaving structures of EQ13 and ER11 are introduced in Figure 3.18 to reduce the AC loss due to proximity effect.

Using Maxwell 2D Field Simulator for input voltage of 36 V (worst case for the transformer copper loss) and switching frequency of 400 kHz, current distributions for the above four structures are computed, as illustrated in Figures 3.19 to 3.21. It can be shown that current distributes more uniformly in the interleaved structures than non-interleaved structures. Maxwell

37

2D simulation results also present the high-frequency copper losses in Watts per unit length.

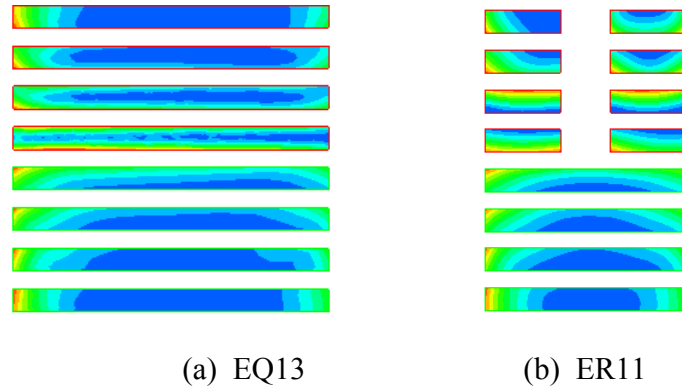Total conduction losses for these four winding arrangements are demonstrated in Figure 3.22.

(a) EQ13   (b) ER11

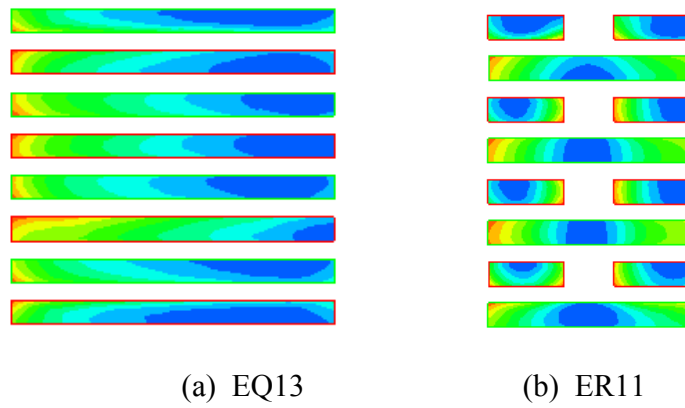Figure 3.19 Current distribution for non-interleaving structure.

(a) EQ13   (b) ER11

Figure 3.20 Current distribution for interleaving structure I.

(a) EQ13   (b) ER11
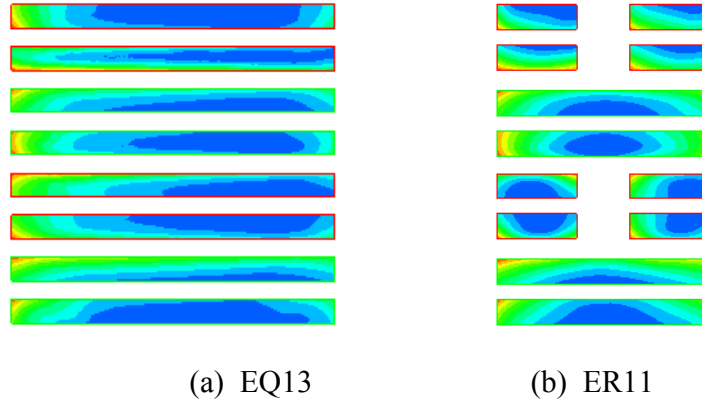
Figure 3.21 Current distribution for interleaving structure II.

EQ13   ER11
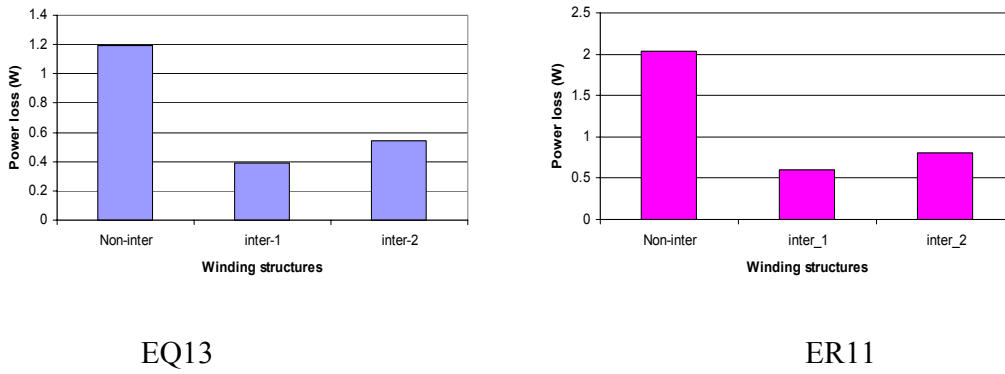
Figure 3.22 Conduction loss comparison.

From the simulated results, it is shown that interleaving primary and secondary windings can dramatically improve the current distribution and therefore significantly reduce the AC copper losses. The conduction loss comparison in Figure 3.22 indicates that the losses for interleaving structure 1 are the smallest among the three interleaving structures.

(3) Maxwell 3D Simulations

It should be noted that the effect of winding terminations and connections in the transformer is neglected in Maxwell 2D simulation. However, un-properly designed connections

and terminations could contribute a significant part of total loss in transformers. In order to accurately calculate AC loss in transformer windings, it is desirable to simulate the conduction losses from 3D point of view.

Figure 3.23 shows the 3D models for the optimized interleaving structures I of ER11 and EQ13. The red windings are primary and the green ones represent secondary windings. Based on the simulation results and current distributions, the optimized connections and terminations can be achieved. Hence, more accurate loss results are obtained.

| (a) | (b) |
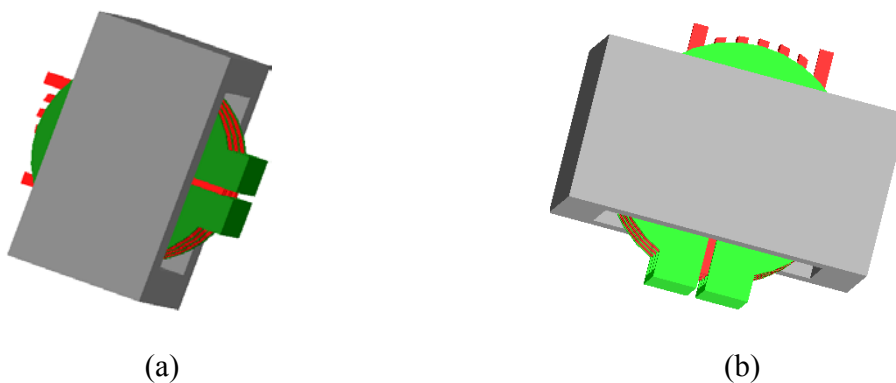
Figure 3.23 3D models of interleaved planar transformers: (a) ER11, and (b) EQ13.

The simulated results for ER11 and EQ13 with interleaving structures I are shown in Figures 3.24 and 3.25.

ER11

Figure 3.24 3D simulation results for ER11.

EQ13

Figure 3.25 3D simulation results for EQ13.

As seen from above curves of 3D simulation results, copper loss decreases as the frequency goes high. This is because the reduction of current ripple results in smaller RMS value of the current. It can then be concluded from the comparisons of 2D and 3D simulations that vias and terminations influence copper loss greatly.

3.2.5 Effect of input voltage on transformer

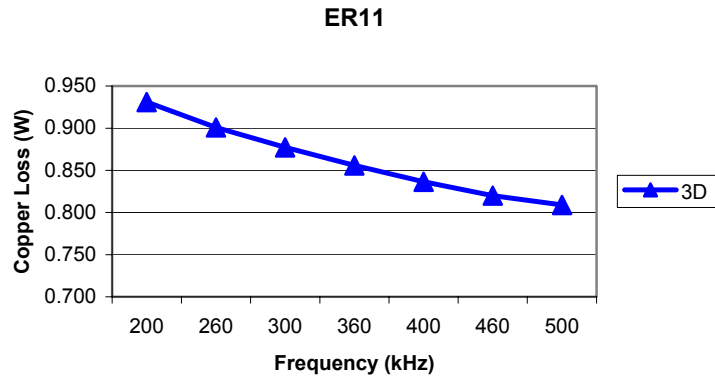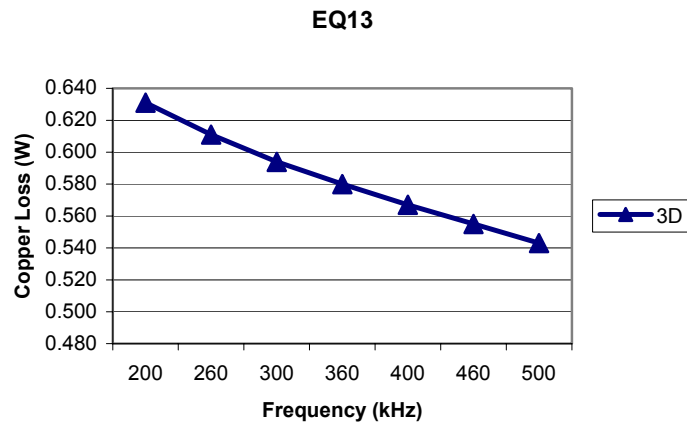After some evaluation and tradeoff of the overall topology at a range of frequencies, we decide the switching frequency to be 400 kHz. Since the input voltage is from 36 V to 75 V, the design work would not be complete without investigation into the effect of input voltage change on the transformer performance. From the expression (3.8) for I_{rms} and duty cycle D,

$$D(V_{in}) = \frac{2 \cdot V_o \cdot N_p}{N_s \cdot V_{in}} \tag{3.13}$$

$$I_{rms} = \sqrt{2} \cdot I \cdot \sqrt{D} \cdot \sqrt{1 + \frac{1}{3} \cdot \left(\frac{\Delta I}{I}\right)^2} \tag{3.14}$$

it is found that the current RMS value decreases with the increase of the input voltage, as illustrated in Figure 3.26 (referred to the secondary for EQ13 and ER11).
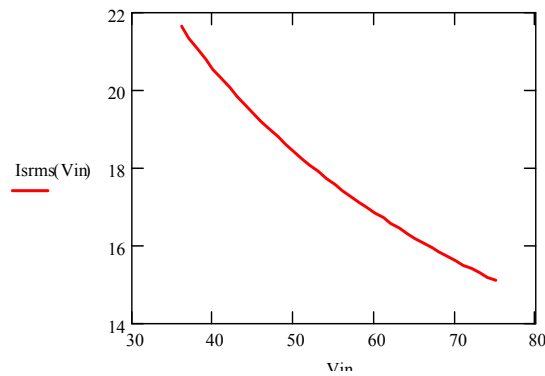

Figure 3.26 RMS value of the secondary current versus input voltage.

Therefore, the reduction of copper loss is expected. Again, FEM simulators are introduced to verify this assumption.

From Maxwell 2D simulation, copper losses for ER11 and EQ13 at different input voltages are shown in Figure 3.27. It is seen that the smaller core ER11 has more copper loss than the larger core EQ13. And for both cores, copper losses decrease with the increase of input voltage. Therefore, the worst case for the transformer is at input voltage of 36 V.
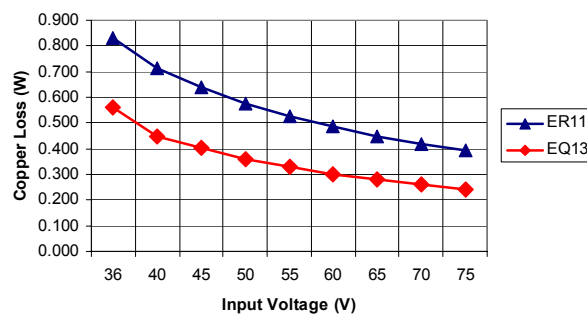
Figure 3.27 Effect of input voltage on copper loss of transformer.

From equations **(**3.6**)** and **(3**.3**)**, the AC flux density and core loss remains stable for a nominal output voltage at a given frequency. This can be verified by Philips software. Therefore, at a specific frequency, the total loss changes only with the RMS values of the currents, i.e., decreases with the increase of the input voltage as shown in Figure 3.28.
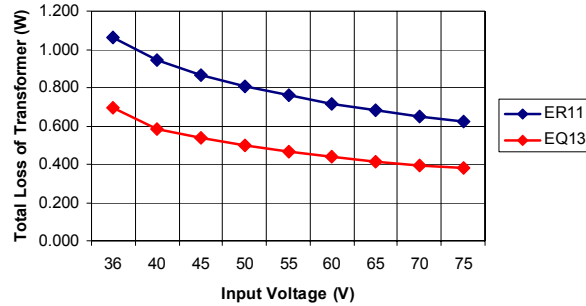
Figure 3.28 Total loss for ER11 and EQ13 at different input voltages.

From efficiency and footprint points of view, we select EQ13 as the transformer core.

3.3 Design of Planar Filter Inductor

Different from the design of transformer, inductor design does not involve interleaving structures to reduce AC losses since there is no secondary winding for interleaving.

To better illustrate the inductor design, the DCS-PWM-based ZVS converter [26] is still employed. The inductor specifications are shown in Table 3.6.

Table 3.6 Specifications for the inductor design.

Converter input voltage (V)	36~75
Converter output voltage (V)	1.2
Output power (W)	60
Switching frequency (kHz)	400
Inductor height (inch)	0.22
Applied current (A)	25+ripple

44

The design platform can be shown in figure 3.29.
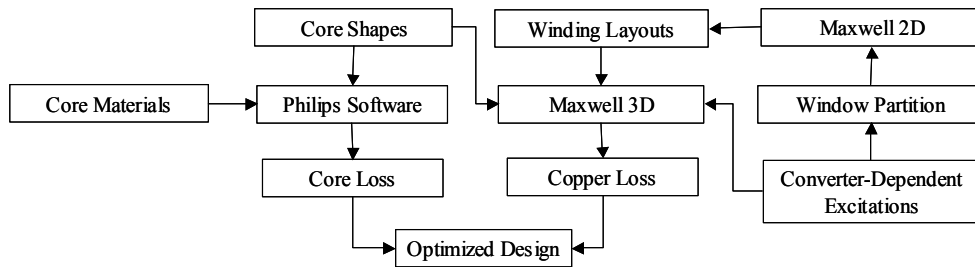
Figure 3.29 Design platform for the inductor.

Similar to the transformer design, the first step is to decide core shapes and core materials. Then core losses are evaluated by Philips software. For copper loss calculation, converter-dependent excitations are used as inputs. After determining the window partition, Maxwell simulators are introduced to obtain the winding layouts, as well as copper loss. Hence, the optimal design is achieved.

3.3.1 Selection of Core Material and Shape

For a given winding, the type of magnetic core material and overall structure of the core clearly have pronounced effects on high-frequency performance. Desirable characteristics of magnetic materials for inductors can be summarized as follows:

- High saturation flux density in order to obtain high saturation current,
- High permeability to obtain high inductance,

- High resistivity to reduce eddy current loss.

The DCS topology has two inductors which are combined to serve as a current doubler to achieve the required 50 A output current, therefore average current for a single inductor is as high as 25 A. To prevent saturation, it is critical to select core materials that have high saturation flux densities. Nevertheless, air-gaps are needed for inductors to prevent saturation. The air-gap length is given by

$$l_g = \frac{\mu_0 \cdot A_c \cdot N^2}{L} \tag{3.15}$$

where A_c is the cross-sectional area of the core, N is the turn number of the winding, and L represents the inductance value. For layout purpose, one turn is assumed.

Carefully investigating main core material vendors, we choose 3F35 and 3F3 as our desired core materials. Although 3F35 has relatively smaller loss density, it is not suitable for operation at frequencies lower than 400 kHz. Therefore, 3F3 is employed for our preliminary design at frequencies below 400 kHz. Just like the transformer, there are four core shapes ER95, ER11, E14, and EQ13 available that meet the height requirement. The specifications for these cores are given in previous sections. The AC flux density of the inductor is given by

$$\Delta B = \frac{V_0 \cdot (1 - D)}{2 \cdot N \cdot A_e \cdot f} \tag{3.16}$$

from which we obtain the core losses for the inductor. Figure 3.30 illustrates the effects of core materials, shapes, and frequency on inductor core loss. The curve drops are due to different materials we adopt for frequency below and above 400 kHz as mentioned in previous sections. Typically, core loss is increased at higher frequencies. At the same time, it can be concluded from Figure 3.30 that the smaller the core is, the larger the core loss would be.
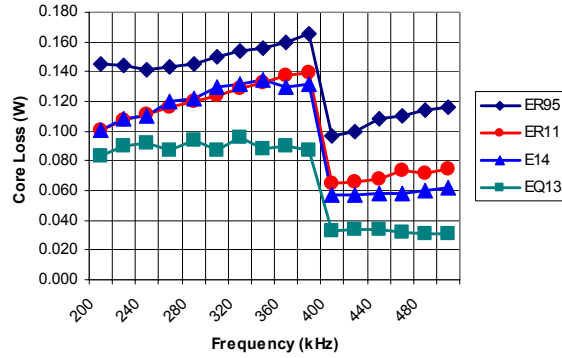
Figure 3.30 Effects of core materials, shapes, and frequency on inductor core loss.

Generally, magnetic component design involves a compromise between the reduction of losses and the expense of increased footprint or vice versa. EQ13 has the smallest core loss but the largest footprint among the candidate cores (see Table 3.2). Therefore, tradeoff still exists in the core selection.

For the same reasons as in the transformer design, E14 is not desirable for the inductor. Also, ER95 is not suitable because the cross-sectional area (A_e) is relatively small. This can be explained clearly from expression

$$L = \frac{\mu \cdot N^2 \cdot A_e}{l_g} \tag{3.17}$$

that the inductance is proportional to A_e. Thus, A_e of ER95 is great enough to reduce the current ripple, since the current ripple is inversely proportional to L as given by

$$\Delta I = \frac{Vo \cdot (1 - D)}{2 \cdot L \cdot f} \tag{3.18}$$

From the topological point of view, large current ripple induces great switching loss. Therefore, ER95 is not evaluated in the following discussions.

47

3.3.2 Total loss of the inductor

To obtain desired inductance value and minimize overall copper loss plus core loss as well, we choose an ER11 and an EQ13 ferrite structures with air-gaps. The copper loss of inductor can be given by equation **(**3.4**),** where

$$I_{rms} = I \cdot \sqrt{1 + \frac{1}{3} \cdot (\frac{\Delta I}{I})^2} \qquad (3.19)$$

Unlike the design of transformer, there is no secondary winding for interleaving. Therefore, Maxwell 3D is applied directly to obtain the copper losses. The 3D models of the inductor are shown in Figure 3.31.

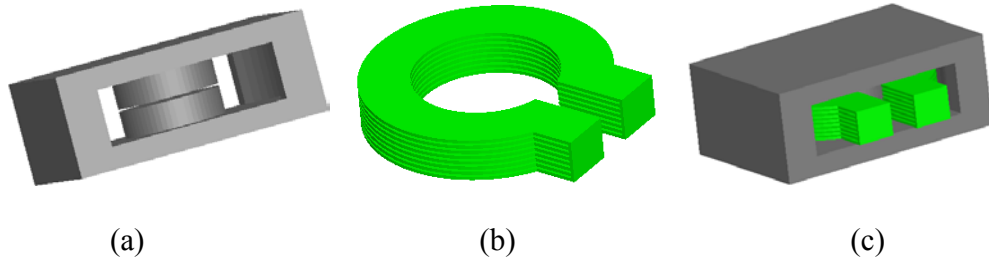| (a) | (b) | (c) |

Figure 3.31 3-D models of the inductor: (a) Core; (b) winding; and (c) overall structure.

At the input voltage of 36 V, Fourier transformed currents are applied to the 3D model. The simulated losses are shown in Figure 3.32.
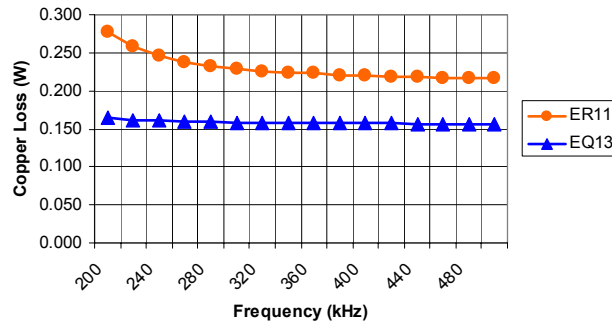
Figure 3.32 Copper losses for ER11 and EQ13.

According to Figure 3.32, change of frequency leads to a little change of copper loss. This can be explained from circuit and magnetic points of view. Generally, as frequency increases, the output current ripple is reduced for a specific inductance value. As a result, the RMS value of the output current is reduced, which causes the decrease of the copper loss. However, the increase of the frequency causes extra ac losses due to skin effect and proximity effect. Consequently, two tendencies compromises to contribute to the total copper loss of the inductor. Combined with the core losses shown in Figure 3.30, the total losses for ER11 and EQ13 are illustrated in Figure 3.33:

Figure 3.33 Total losses for ER11 and EQ13.

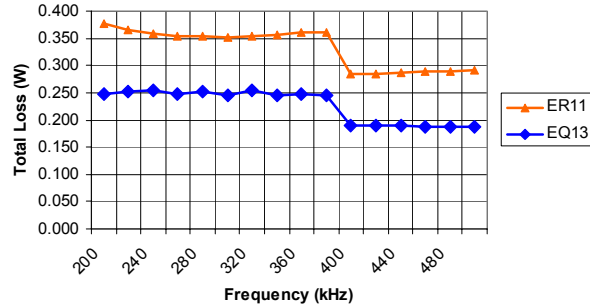Figure 3.33 suggests that frequency change doesn't affect total loss significantly for a given core shape with a specific material. And within a range of frequencies, the larger the core is, the smaller the total loss will be. Also due to different loss density of 3F3 and 3F35, significant curve drops can be found around frequency of 400 kHz.

It has been proved that the worst case for the transformer at a given frequency is at 36 V input voltage. In order to see the effect of input voltage on copper loss of the inductor, we first look at the equation for the duty cycle

$$D(V_{in}) = \frac{2 \cdot V_o \cdot N_p}{N_s \cdot V_{in}} \tag{3.20}$$

from which we found that the duty cycle $D(V_{in})$ decreases with the increase of input voltage. Therefore, the current ripple

$$\Delta I = \frac{Vo \cdot (1 - D(V_{in}))}{2 \cdot L \cdot f} \tag{3.21}$$

will increase as the input voltage increases in case the frequency is fixed. However, the ripple is so small that significant change of RMS current value is not expected according to (3.19), which leads to negligible change of copper loss as shown in Figure 2.34.

50
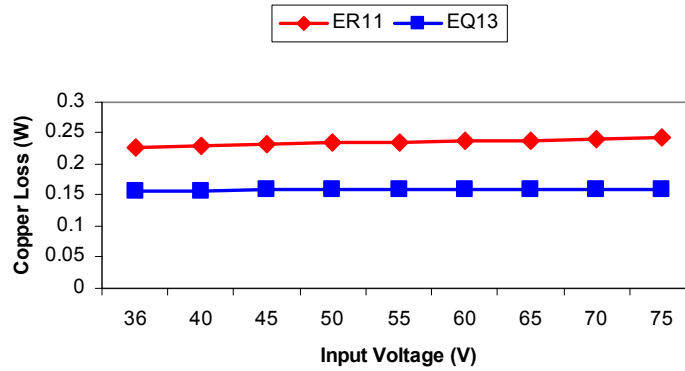
Figure 3.34 Copper loss vs input voltage

According to equation (3.16), increase of the input voltage results in increase of AC flux density, which leads to the increment of core loss as shown in Figure 3.35. The input voltage is set to be from 36 V to 75 V.
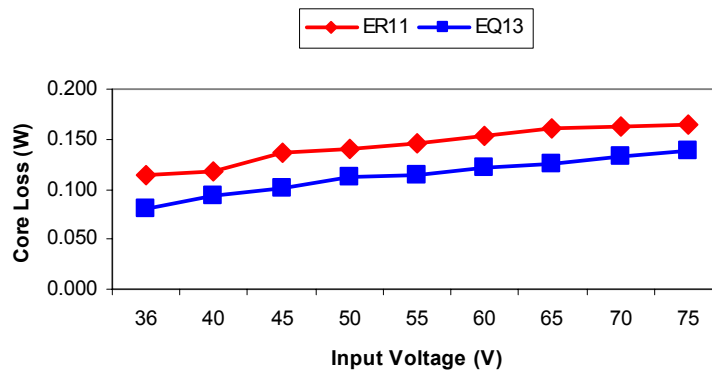
Figure 3.35 Core loss vs input voltage.

Figure 3.36 is obtained by combining Figures 3.34 and 3.35. Notice that different from the transformer, the inductor has the smallest loss at the 36V input voltage, and the total loss increase as the voltage goes high.
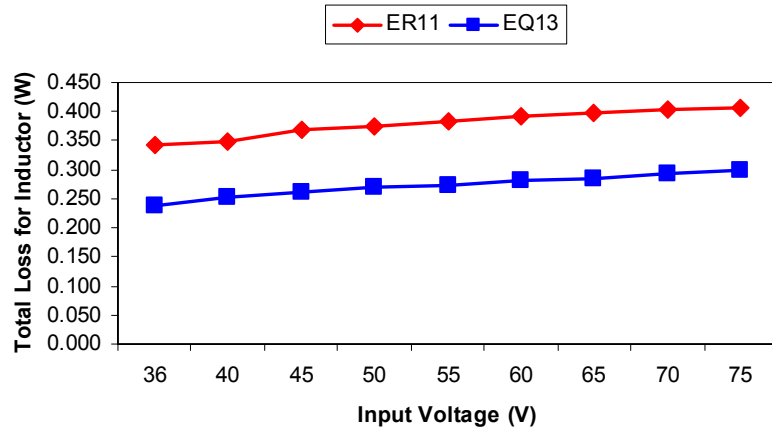
Figure 3.36 Total loss for the inductor at different input voltages.

3.4 Design results

Carefully budgeting layout and power loss by evaluation of the total topology, we decide the core shape for the transformer to be EQ13, and the inductors ER11. The core material is 3F35. Then the preliminary design results of magnetics on 8-layer PCB can be summarized as shown in Table 3.7.

Table 3.7 Design summary of planar magnetics.

|	Transformer		Inductor	Thickness (μm)
	Layers	Turns	Layers	
	Solder mask		Solder mask	50
1	Secondary	1	Winding	70
	Insulation		Insulation	130
2	Primary	1	Winding	140
	Insulation		Insulation	130
3	Secondary	1	Winding	140
	Insulation		Insulation	130
4	Primary	1	Winding	140
	Insulation		Insulation	130
5	Secondary	1	Winding	140
	Insulation		Insulation	130
6	Primary	1	Winding	140
	Insulation		Insulation	130
7	Secondary	1	Winding	140
	Insulation		Insulation	130
8	Primary	1	Winding	70
	Solder mask		Solder mask	50
Total				1990

From the measurement, the total footprint for the magnetics is around 334mm^2. At the design switching frequency of 400 kHz, the effect of input voltage on losses for the transformer and two inductors can be summarized as follows:
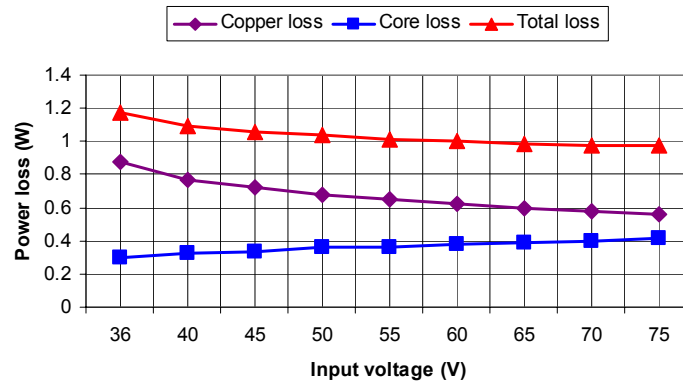
Figure 3.37 Magnetic losses versus input voltage.

Examining the above figure, we find that core loss is increased as the input voltage increases. In contrast, copper loss decreases a larger amount with the increase of input voltage. As a result, total loss decreases with the increase of input voltage.

4 CONCLUSION

A novel design methodology of planar magnetics based on numerical analysis of electromagnetic fields is proposed and successfully applied to the design of low-voltage high power density dc-dc converters. The design methodology features intense use of FEM simulation. As a powerful simulation software for electromagnetic analysis, Maxwell 2D delivers virtual prototypes of magnetics quickly and accurately. Throughout this thesis, Maxwell 2D field simulator is effectively adopted to obtain optimal interleaving structures. It is also proved that poor via and termination design can offset merits brought by carefully designed windings. Thus, 3D simulator is indispensable to optimize the whole winding layout. Maxwell 3D can simulate frequency and time domain electromagnetic fields in complex 3D structures with unsurpassed accuracy and ease of use. It is therefore employed throughout the design for magnetics in this thesis.

Effects of input voltage, core shape, and frequency on magnetics are investigated. While the transformer core loss is insensitive to the input voltage, the inductor copper loss is reluctant to change with the input voltage at a given frequency. If the total loss is evaluated, the worst case is found to be at the lowest input voltage for the transformer. On the contrary, the worst case for the inductor is at the highest input voltage. Based on the core shape samples, it is found that larger core has larger losses for both transformer and inductor. In the specified frequency range, losses for the transformer and inductor are reduced with the increase of the frequency.

Through the study, it is demonstrated that ac losses play dominant roles in magnetics design at high frequencies. For the transformer, interleaving primary and secondary windings can dramatically improve the current distribution and therefore significantly reduce the ac copper losses that are difficult to be accounted for by conventional design methods. In contrast, no interleaving structure is available for the inductor design. Therefore, more attention should be focused on the selection of core shape and material.

LIST OF REFERENCES

[1] C. Quinn, K. Rinne, T. O'Donnell, M. Duffy, and C. O. Mathuna: A review of planar magnetic techniques and technologies. IEEE APEC'2001, Vol. 2, pp: 1175-1183

[2] M. Rascon, J. Ara, R. Madsen, J. Navas, M. Perez, and F. San Miguel: Thermal analysis and modelling of planar magnetic components. IEEE APEC'2001, Vol. 1, pp. 97 -101

[3] P. D. Evans, and W. J. B. Heffernan: Multi-megahertz transformers. IEEE IAS'1995, Vol. 1, pp. 824 -832

[4] Bo Yang, Rengang Chen, and F. C. Lee: Integrated magnetic for LLC resonant converter. IEEE APEC'2002, Vol. 1, pp. 346-351

[5] Leung-Pong Wong, Yim-Shu Lee, and David Ki-Wai Cheng: A new approach to the analysis and design of integrated magnetics. IEEE APEC'2001, Vol. 2, pp. 1196-1202

[6] K. Wallace: Multiple output planar transformer. IBM Technical Disclosure Bulletin, Vol. 24, No. 8, Jan. 1982

[7] Anon.: Split plate transformer. IBM Technical Disclosure Bulletin, Vol. 28, No. 2, July 1985, pp. 625-626

[8] Anon.: New magnetic structure for a low profile planar transformer. IBM Technical Disclosure Bulletin, March 1986, pp. 4245-4247

[9] A. Estrov: Power transformer design for 1MHz resonant converter. High Frequency Power Conversion Proceedings, May 1986, pp. 36-54

[10] P. M. Gradski and Fred C. Lee: Design of high frequency hybrid power transformer. IEEE APEC 1988.

[11] L. F. Casey, M. F. Schlecht: A high frequency, low volume point-of -load power supply for distributed power systems. IEEE Trans. Power Electronics, Vol. 3, No. 1, pp. 72-82, 1988

[12] M. T. Quirke, J. J. Barret, M. Hayes: Planar magnetic component technology- a review. IEEE Trans. Comp. Hybrids, and Man. Tech., October 1992, pp. 884-892

[13] P. G. Barnwell, T. J. Jackson: High frequency transformers using thick film technology. 8th European Hybrid Microelectronics Conference 1991, pp. 21 1-218

[14] P. G. Barnwell, T. J. Jackson: Low profile high frequency power supplies using thick film planar transformers. EPE Sept.1993, pp.93-97

[15] R. J. Huljak, V. J. Thottuvelil, A. J. Marsh, B. A. Miller: Where are power supplies headed. IEEE APEC 2000, pp. 10-17.

[16] N. Dai, A. W. Lotfi, G. Skutt, W Tabisz, F. C. Lee: A comparative study of high frequency low profile planar transformer technologies. IEEE APEC'94, pp.153 - 161

[17] Philips Magnetic Components: Design of Planar Power Transformers. Application Note

[18] K. D. T. Ngo, R. S. Lai: Effect of height on power density in spiral-wound power-pot-core transformers. IEEE Trans. Power Elec. Vol. 7. No.3.Jul 1992

[19] Prieto, R., Garcia, O., Asensi, R., Cobos, J.a., Uceda, J.: Optimizing the performance of planar transformers. IEEE APEC '96. Vol. 1, pp: 415-421

[20] S. Ramakrishnan, R. Steigerwald, J. A. Mallick: A comparison study of low-profile power magnetics for high frequency high density switching converters. IEEE APEC 97, pp 415-421

[21] N. Dai, F. C. Lee: Edge effect analysis in high frequency transformer. IEEE PESC'94, pp.850-855

[22] X. Huang, K. D. T. Ngo, G. Bloom: Design techniques for planar windings with low resistances. IEEE APEC'95, pp.533-539

[23] P. L. Dowell: Effect of eddy currents in transformer windings. IEE, vol.113, No.8. Aug 1966

[24] G. Skutt, F. C. Lee, R. Ridley and D. Nicol: Leakage inductance and termination effects in a high-power planar magnetic structure. IEEE APEC'94, pp.295-301

[25] Robert W. Erickson and Dragan Maksimovic: Fundamentals of power electronics, 2nd edition.

[26] Quarterly Report #1 for ASTEC Power/Emerson, High-Density Low-Voltage DC-DC Converters with Improved Efficiency and Increased Power Density, February 2003

[27] Application Note, Design of Planar Power Transformer, www.ferroxcube.com.

[28] Liming Ye, G. R. Skutt, R. Wolf, F.C Lee: Improved winding design for planar inductors. IEEE PESC'97, Vol. 2, pp. 1561-1567